HHS Public Access

Author manuscript

Kidney Int. Author manuscript; available in PMC 2014 September 01.

Published in final edited form as:

Kidney Int. 2014 March ; 85(3): 561–569. doi:10.1038/ki.2013.397.

Increased mitochondrial activity in renal proximal tubule cells from young spontaneously hypertensive rats

Hewang Lee[1,*,2], **Yoshifusa Abe**[2], **Icksoo Lee**[3], **Shashi Shrivastav**[2], **Annabelle P. Crusan**[1], **Maik Hüttemann**[4], **Ulrich Hopfer**[5], **Robin A. Felder**[6], **Laureano D. Asico**[1], **Ines Armando**[1], **Pedro A. Jose**[1,#], and **Jeffrey B. Kopp**[2,#]

[1]Division of Nephrology, Department of Medicine, University of Maryland School of Medicine, Baltimore, MD 21201

[2]Kidney Disease Section, Kidney Disease Branch, National Institute of Diabetes and Digestive and Kidney Diseases, National Institutes of Health, Bethesda, MD 20892

[3]College of Medicine, Dankook University, Cheonan-si, Chungcheongnam-do, 330-714, Korea

[4]Center for Molecular Medicine and Genetics and Cardiovascular Research Institute, Wayne State University School of Medicine, Detroit, MI 48201

[5]Department of Physiology and Biophysics, Case Western Reserve University, School of Medicine, Cleveland, OH 44106

[6]Department of Pathology, University of Virginia Health Sciences Center, Charlottesville, VA 22908

Abstract

Renal proximal tubule cells from spontaneously hypertensive rats (SHR), compared with normotensive Wistar-Kyoto rats (WKY), have increased oxidative stress. The contribution of mitochondrial oxidative phosphorylation to the subsequent hypertensive phenotype remains unclear. We found that renal proximal tubule cells from SHR, relative to WKY, had significantly higher basal oxygen consumption rates, ATP synthesis-linked oxygen consumption rates, and maximum and reserve respiration. These bioenergetic parameters indicated increased mitochondrial function in renal proximal tubule cells from SHR compared with WKY. Pyruvate dehydrogenase complex activity was consistently higher in both renal proximal tubule cells and cortical homogenates from SHR than WKY. Treatment for 6 days with dichloroacetate, an inhibitor of pyruvate dehydrogenase kinase, significantly increased renal pyruvate dehydrogenase complex activity and systolic blood pressure in 3-week old WKY and SHR. Therefore, mitochondrial oxidative phosphorylation is higher in renal proximal tubule cells from SHR

[*]Corresponding author Hewang Lee, PhD, 10 Center Dr, 3N114, Bethesda MD 20892-1268, lih14@mail.nih.gov, Fax: 301-402-0014, Tel: 301-496-3116.

[#]Senior authors

DISCLOSURE

All the authors declared no competing interests.

Supplementary information is available at *Kidney International*'s website.

compared with WKY. Thus the pyruvate dehydrogenase complex is a determinant of increased mitochondrial metabolism that could be a causal contributor to the hypertension in SHR.

Keywords

oxygen consumption rate; pyruvate dehydrogenase complex; mitochondria; systolic blood pressure; renal proximal tubule

INTRODUCTION

Essential hypertension is a heterogeneous disorder in which both genetics and environmental factors contribute to increased cardiovascular and renal morbidity and mortality. [1,2] The importance of the renal proximal tubule in the pathogenesis of hypertension, especially polygenic or essential, has recently being appreciated.[1,3] Selective deletion in the renal proximal tubule of aromatic amino acid decarboxylase, the enzyme that converts L-3,4-dihydroxyphenylalanine to dopamine, causes salt-sensitive hypertension in mice.[4] Conversely, selective deletion of angiotensin type I_A receptor in the renal proximal tubule reduces sodium transport in this nephron segment, decreases sodium balance, and protects against angiotensin II- and salt-induced hypertension in mice.[5]

Renal proximal tubule cells and cortical homogenates from spontaneously hypertensive rats (SHR), compared with normotensive Wistar-Kyoto rats (WKY), have increased oxidative stress, [6, 7] which may contribute to the increased renal tubular sodium reabsorption.[1,3, 6] The association of the increased activity of nicotinamide adenine dinucleotide phosphate (NADPH) oxidase with hypertension is well established,[6, 8] but the importance of renal mitochondria-derived reactive oxygen species in hypertension has only recently been recognized. [9-11] Zhang et al [9] have reported that the mitochondrial respiratory chain is a major source of oxidative stress in mice with deoxycorticosterone acetate salt-induced hypertension. In stroke-prone SHR, the mitochondria-targeted antioxidant MitoQ10 protects against the development of hypertension.[10] The above reports suggest that mitochondrial reactive oxygen species are important in the development of hypertension.

The major function of mitochondria is to produce adenosine triphosphate (ATP) to supply energy for various cellular functions, with reactive oxygen species as by-products. The level of mitochondrial ATP production is often reflected by the mitochondrial oxygen consumption rate (OCR).[12] Previous studies have shown that renal proximal tubules from SHR have increased OCR compared with normotensive WKY,[13] however, the molecular mechanisms underlying this difference between WKY and SHR are not well understood.

The mitochondrial pyruvate dehydrogenase complex catalyzes the decarboxylation of pyruvate to acetyl-coenzyme A.[14] The reaction is regulated by reversible phosphorylation of the E1 subunit via pyruvate dehydrogenase kinase and dephosphorylation via pyruvate dehydrogenase phosphatase.[15] The activity of pyruvate dehydrogenase kinase is inhibited by pyruvate and its analogs. Dichloroacetate (DCA), a pyruvate analog and competitive inhibitor of pyruvate dehydrogenase kinase, is used widely to increase pyruvate dehydrogenase complex activity.[14]

To explore the potential molecular mechanisms involved in the increased OCR and mitochondrial function in the SHR, we identified that increased activity of the pyruvate dehydrogenase complex contributes to the pathogenesis of hypertension in this animal model.

RESULTS

Characterization of renal proximal tubule cells in primary culture

We isolated proximal tubules from rat kidneys. The purity of renal proximal tubule cells in primary culture was determined by western blot and immunofluorescence. Contaminating renal cells derived from nephron segments distal to the proximal tubule were detected by antibodies against Na^+-K^+-$2Cl^-$cotransporter (NKCC2, Slc12a1), Na^+-Cl^-cotransporter (NCC, Slc12a3), and epithelial sodium channel (ENaC, Scnn1) (Supplementary Figure S1a). Immunofluorescence staining with sodium-glucose linked transporter 2 (SGLT2, Slc5a2) (Supplementary Figure S1b) showed that 92.3-96.0% of cells were positive for this renal proximal tubule cell marker. Although these cells were not 100% renal proximal tubule in origin, we refer to them as renal proximal tubule cells in primary culture for the purpose of this study.

Bioenergetic profiles of renal proximal tubule cells from WKY and SHR

Using the Seahorse Bioscience XF24 Extracellular Flux Analyzer, we studied the OCR response to several mitochondrial inhibitors, [16, 17] including oligomycin (ATP synthase inhibitor), carbonyl cyanide p-trifluoromethoxyphenylhydrazone (FCCP, uncoupler), rotenone (Complex I inhibitor), and antimycin A (Complex III inhibitor) in renal proximal tubule cells isolated from WKY and SHR (Supplementary Figure S2).

Renal proximal tubule cells in primary culture from SHR, compared with normotensive WKY, displayed a distinct bioenergetic profile (Figure 1a). Basal OCR was significantly higher in SHR than WKY (223.7±20.9 vs. 151.0±6.6 pmol/min per 20,000 cells, n=8-9, $P<0.001$) (Figure 1b). ATP synthesis-linked OCR was also greater in SHR than WKY (75.6±7.5% vs. 60.1±4.4% of basal OCR, n=9, $P<0.01$) (Figure 1c). FCCP increased OCR in cells from both rat strains, but the increase was greater in SHR than WKY (418.9±21.4 vs. 252.6±18.1 pmol/min per 20,000 cells, n=8-9, $P<0.001$) (Figure 1d). Similar to the maximum respiration, the reserve respiration was greater in SHR than WKY (88.2±13.6 vs. 67.5±14.2% of basal OCR, n=8-9, $P<0.05$) (Figure 1e). Proton leak-linked OCR tended to be lower in SHR than WKY (10.3±7.9% vs. 19.1±11.4% of basal OCR, n=8-9, $P=0.08$) (Figure 1f) but non-mitochondrial respiration was similar (37.4±20.6 vs. 31.5±13.1 pmol/min per 20,000 cells, n=8-9, $P>0.05$) in the two rat strains (Figure 1g). These results suggest that renal proximal tubule cells in primary culture from SHR have higher mitochondrial function than those from WKY. Similar distinct bioenergetics profile also exists in immortalized cells [18] from SHR, compared with WKY, with higher basal OCR, ATP synthesis-linked OCR, maximum respiration, and reserve respiration (data not shown). Of note, the mitochondrial inhibitors, in the concentrations used, had no effect on cell viability (Supplementary Figure S3).

Glycolysis in renal proximal tubule cells from WKY and SHR

Both primary (Figure 2a) and immortalized (data now shown) renal proximal tubule cells from SHR, relative to WKY, had higher basal extracellular acidification rate (ECAR) (9.29 ±1.5 vs. 2.94±0.7 mpH/min/20,000 primary cells, n=12-16, P<0.001), indicating greater anaerobic glycolysis. Inhibition of mitochondrial function by oligomycin, FCCP, and combination of rotenone and antimycin A increased ECAR in primary (Figure 2a) and immortalized (data now shown) renal proximal tubule cells from both rat strains, but the increase was greater in SHR than WKY, indicating the potential for increased compensatory anaerobic glycolysis in SHR.

Although ECAR is reflective of the level of glycolysis, any metabolic acid secreted from cells contributes to the values of ECAR. [16] Therefore, we measured lactate production in whole kidney homogenates from WKY and SHR. As shown in Figure 2b, lactate production was higher in SHR than WKY, indicating higher glycolysis in former than in the latter rat strain.

ATP level in renal proximal tubule cells from WKY and SHR

Because the foregoing data suggested higher mitochondrial function in renal proximal tubule cells from SHR than those from WKY, we next measured the intracellular ATP concentration. As shown in Figure 3, ATP levels were significantly higher in renal proximal tubule cells from SHR than those from WKY.

Mitochondrial characterization in renal proximal tubule cells from WKY and SHR

We next examined mitochondrial abundance in renal proximal tubule cells by both fluorescence confocal (Figure 4a-4f) and transmission electron (Figure 4g-4j) microscopy. Renal proximal tubule cells in primary culture, which were stained with MitoTracker, showed similar fluorescence density between WKY and SHR (Figure 4k). The mitochondrial number (Figure 4l), size, morphology, distribution of cristae, electron density of the matrix, and the inner and outer mitochondrial membranes (Figure 4h, 4j) in renal proximal tubule cells were similar in WKY and SHR.

The mRNA expressions of glyceraldehyde 3-phosphate dehydrogenase (GAPDH, a glycolytic protein in the cytosol), Complex III core 2 protein (a nuclear genome-encoded mitochondrial protein), and ATP synthase F_0 subunit 6 (a mitochondrial genome-encoded protein) were similar in renal proximal tubule cells in primary culture from these two rat strains (Figure 4m). The protein expression of Complex III core 2 subunit was also similar in immortalized renal proximal tubule cells from WKY and SHR (Figure 5b).

Pyruvate dehydrogenase complex protein expression in renal proximal tubule from WKY and SHR

The increased oxidative phosphorylation and glycolysis in renal proximal tubule cells from SHR prompted us to explore the molecular mechanisms at the interface between glycolysis and oxidative phosphorylation. Pyruvate dehydrogenase complex is one such candidate that plays a crucial role in linking glycolysis and gluconeogenesis in the cytosol with the tricarboxylic acid cycle and subsequent oxidative phosphorylation in the mitochondria. [14, 15]

We, therefore, measured the level of pyruvate dehydrogenase complex protein expression and activity in WKY and SHR. Compared with renal proximal tubule cells from WKY, the cells from SHR had higher E2/3 binding protein expression (Figure 5a) while the protein expression of lactate dehydrogenase and Complex III core 2 subunit were similar in the cells from these two rat strains (Figure 5b).

We also measured pyruvate dehydrogenase complex protein expression in renal cortical homogenates from 3-8 week old WKY and SHR. Similar to the findings in the renal proximal tubule cells, the protein expression of E2/3 binding protein in renal cortical homogenates was significantly higher in SHR than WKY (Figure 5c).

Pyruvate dehydrogenase complex activity in renal proximal tubule from WKY and SHR

The increased pyruvate dehydrogenase complex protein expression in SHR, compared with WKY, was associated with increased pyruvate dehydrogenase complex activity in renal proximal tubule cells (4.21±1.0 vs. 1.81±0.4 ΔmOD450 nm/min/mg protein, $P<0.05$) (Figure 6a), renal cortical homogenates (14.28±2.1 vs. 9.91±1.2 ΔmOD450 nm/min/mg protein, $P<0.05$) (Figure 6b), and whole kidney homogenates (1.58±0.13 vs. 1.13±0.09 ΔmOD_{450}/mg protein/min, $P<0.05$) (Figure 6c).

To assess whether or not DCA, a pyruvate dehydrogenase kinase inhibitor, increased renal pyruvate dehydrogenase complex activity, pyruvate dehydrogenase activity was measured. As shown in Figure 6c, DCA increased the pyruvate dehydrogenase complex activity in kidney homogenates from both WKY (1.57±0.30 vs. 1.13±0.09 ΔmOD_{450}/mg protein/min, $P<0.05$) and SHR (2.40±0.36 vs. 1.58±0.13 ΔmOD_{450}/mg protein/min, $P<0.05$). Of note, pyruvate dehydrogenase complex activity which was higher in the basal state in SHR than WKY, remained higher after DCA treatment.

Blood pressure in DCA-treated young WKY and SHR

We next measured blood pressure in young WKY and SHR treated with DCA. Before DCA treatment, at age of 22 days, blood pressure was not different in WKY (92.7±2.6 vs. 93.6±2.4 mmHg, n=10-11, $P>0.05$) and SHR (100.2±4.5 vs. 100.6±4.4 mmHg, n=9-11, $P>0.05$). One-day of DCA treatment did not significantly change the blood pressure in both WKY and SHR. After 6 days of DCA treatment, systolic blood pressure, significantly increased in both WKY (101.2±2.6 vs. 112.6±1.9 mmHg, n=10-11, $P<0.05$) and SHR (112.3±2.3 vs. 126.8±4.0 mmHg, n=9-11, $P<0.05$) but continued to be higher in SHR than WKY (Figure 7). Of note, systolic blood pressure was higher at age of 29 days in untreated SHR than WKY.

DISCUSSION

The SHR is one of the most extensively investigated animal models in the study of essential hypertension.[7,18,19-21] SHRs have slightly higher blood pressure than WKYs at birth but develop sustained hypertension after 8 weeks of age.[19-21] In the current study, using the tail-cuff method, the blood pressure was significantly higher at 29 days of age in SHR as compared with WKY (Figure 7). The causes of the hypertensive phenotype of the SHR are not well understood, but may be related to differences in the expression of several genes

under genetic and epigenetic control.[22, 23] In the present study, we observed that renal proximal tubule cells from SHR, compared with WKY, had higher basal OCR (Figure 1), indicating higher oxygen expenditure, which is consistent with previous reports of increased oxidative metabolism and lower utilization efficiency of O_2 in renal cortical tubules from SHR. [12,13] The higher ATP synthesis-linked OCR, maximum respiration, and reserve respiration (Figure 1) indicate increased mitochondrial function in renal proximal tubule cells from SHR, consistent with higher ATP production in these cells from SHR than those from WKY (Figure 3). The stable phenotypic difference of OCR in renal proximal tubule cells between WKY and SHR, not caused by an increase in the amount or volume of mitochondria (Figure 4), is probably related to an epigenetically or genetically programmed increase in sodium transport, or intrinsic genetic differences between these two rat strains. [22, 23]

Fumarate, a tricarboxylic acid cycle product, is higher in the kidney of Dahl-salt sensitive than normotensive Brown Norway rats.[11] Succinate, another tricarboxylic acid cycle product, has been reported to increase blood pressure in Sprague-Dawley rats.[24] The increased energy metabolism in some hypertensive animal models [11, 24] is in contrast with reports that energy metabolism is impaired in other hypertensive animal models.[25, 26] The discrepancy may be caused by different tissue/organ specific protein-metabolite interaction [27] or different stages of development. [28]

The increased oxygen consumption and energy metabolism in SHR are supported by the observation of increased pyruvate dehydrogenase complex activity in renal proximal tubule cells from SHR compared with WKY (Figure 6). The pyruvate dehydrogenase complex catalyzes the conversion of pyruvate to acetyl-coenzyme A.[14, 15] Pyruvate, a critical substrate for energy metabolism, is derived mainly from glycolysis and catabolism of certain amino acids; acetyl-coenzyme A enters the tricarboxylic acid cycle for subsequent oxygen-dependent energy production through the electron transport chain. The higher ECAR levels and lactate production (Figure 2) in renal proximal tubule cells from SHR, relative to WKY, and the increase in pyruvate dehydrogenase complex activity (Figure 6), indicate a higher rate of pyruvate flux into the tricarboxylic acid cycle, and subsequent increased oxidative phosphorylation in SHR. These differences in proximal tubule phenotype must reflect strain-specific changes in gene expression intrinsic to this tissue, as opposed to proximal tubule responses to cues from other parts of the body, because similar strain-specific metabolic changes were observed in primary proximal tubule cells, cortical homogenates, and immortalized cell lines from SHR versus WKY.

The role of energy metabolism in the pathogenesis of hypertension has not been widely appreciated. The finding that DCA increased pyruvate dehydrogenase complex activity (Figure 6c) and blood pressure (Figure 7) in both WKY and SHR provides mechanistic evidence that increased activity of pyruvate dehydrogenase complex is a causal contributor to hypertension. Previous studies have shown that the young SHR has enhanced sodium transport in renal proximal tubules, relative to age-matched control WKY. [29-31] Presumably, the increased renal oxygen consumption in the SHR is the result of enhanced basal activity of pyruvate dehydrogenase complex (in association with other enzymes and substrates of energy metabolism), that facilitates the conversion of pyruvate to acetyl-coenzyme A and

accelerates the activity of the tricarboxylic acid cycle and oxidative phosphorylation. An increase in glycolysis also provides more sources of fuel, e.g., pyruvate. A recent proteomic study [32] showed that voltage-dependent anion selective channel (VDAC) 2 protein expression was higher in salt-sensitive hypertensive than normotensive Brown Norway rats. The increase in VDAC 2 protein expression and activity could provide a mechanism for an increase in the flux of metabolites, including pyruvate from cytosol into mitochondria, [33, 34] which results in increased activity of the tricarboxylic acid cycle and mitochondrial energy metabolism. The increase in both oxidative phosphorylation and glycolysis results in enhanced ATP production to meet the energy demand for increased sodium transport (and possibly other solutes) in the proximal tubule (and possibly other nephron segments), which is consistent with previous studies showing that renal oxygen consumption for sodium transport is higher in SHR than WKY. [12] The increased renal pyruvate dehydrogenase complex activity in SHR, found in the current study, may be one mechanism that contributes to increased renal sodium transport and subsequent development of hypertension.

Another mechanism for the increased renal sodium transport and blood pressure in the SHR, that may be related to or independent of increased renal pyruvate dehydrogenase complex activity, is the increase in the production of reactive oxygen species.[6-11,35-37] For example, both NADPH oxidase- and mitochondria-derived reactive oxygen species are higher in kidneys of SHR than WKY.[6-11,37] DCA, which increases pyruvate dehydrogenase complex activity, has been reported to augment reactive oxygen species production in many cell types.[38,39] The intravenous infusion of fumarate increases reactive oxygen species production in the renal medulla and exacerbates the salt-induced hypertension in Dahl salt-sensitive rats.[11] The increase in reactive oxygen species production, per se or in association with the increase in renal sodium transport, could be another mechanism for the pyruvate dehydrogenase complex-mediated increase in blood pressure. However, additional investigations are needed for the direct proof of a role of pyruvate dehydrogenase complex on renal proximal sodium transport and blood pressure.

In summary, renal proximal tubule cells derived from young SHR, compared with normotensive WKY, have higher basal OCR, maximum and reserve respiration, and greater pyruvate dehydrogenase complex protein expression and activity and ATP production, which suggest greater mitochondrial function. DCA increases renal pyruvate dehydrogenase complex activity and blood pressure in both WKY and SHR, but both variables remain higher in SHR than WKY. The present study provides evidence of an altered bioenergetics profile and energy metabolism in renal proximal tubule cells from a hypertensive rat model, i.e., SHR, and suggests that the pyruvate dehydrogenase complex could be one of the genetic mechanisms that contribute to the pathogenesis of hypertension.

METHODS

Detailed methods are available online at *Kidney International*'s website.

Animals

Male WKY and SHR were purchased from Charles River (Boston, MA) and had free access to food and drinking water. Study protocols and the use of the animals were approved by the NIDDK and the University of Maryland Animal Care and Use Committees.

Isolation of renal proximal tubule and cell culture

Rat renal proximal tubule segments were isolated from WKY and SHR as described previously. [7] The proximal tubule origin of cultured cells was characterized by their expression of proximal tubule marker proteins.

OCR and ECAR measurement

OCR and ECAR were measured by the Seahorse Bioscience XF24-3 Extracellular Flux Analyzer (Seahorse Bioscience), based on the fluorometric detection of O_2 and pH levels.[16,17] Immortalized renal proximal tubule cells [18] were initially employed to obtain the optimal experimental conditions for rat renal proximal tubule cells.

Confocal immunofluorescence microscopy

Fixed renal proximal tubule cells in primary culture (Passage 3) on coverslips were stained with 3 μg/mL anti-SGLT2 IgG following with Alexa Fluor-488 anti-rabbit secondary antibodies.

Mitochondria in live renal proximal tubule cells in primary culture (Passage 3) were stained with MitoTracker Green (Invitrogen, Eugene, OR). The three-dimensional (3D) restoration and imaging analysis were conducted using the built-in ZEN 2011 software.

Electron microscopy

Transmission electron microscopy was performed as described previously. [40] Briefly, kidney tissue samples were fixed in 4F1G solution [40] for 24 hr and then postfixed in osmium tetroxide, dehydrated in graded alcohols, and embedded in epoxy resin. After the proximal tubules were identified in the thick sections, ultrathin sections were stained with 0.5% uranyl acetate and 1% lead citrate, mounted on grids, and examined on a JEM 1200 transmission electron microscope. Mitochondria were counted from fifteen to twenty randomly selected fields at 3,000× magnification from both WKY and SHR kidney tissues. Mitochondrial morphology was observed under 15,000× to 20,000× magnification.

Quantitative real-time PCR

Total RNA was extracted from renal proximal tubule cells in primary culture, using NucleoSpin RNA kit (Clontech, Mountain View, CA). Total RNA samples (1μg) were reverse-transcribed using GoScript reverse transcriptase (Promega, Madison, WI). The real-time PCR reaction containing SYBR Green PCR Master Mix was added in 10 μl per well in a 384-well optical plate, and was performed in the 7500 Real-time PCR System (Applied Biosystems). Data were analyzed using the comparative ΔCt method for calculating relative gene expression. [41]

ATP quantification

In vitro ATP concentration was measured using the ATP bioluminescence assay kit HS II (Roche Applied Science, Indianapolis, IN) following the manufacturer's instructions as described previously.[42]

Pyruvate dehydrogenase complex activity assay

In vitro pyruvate dehydrogenase complex activity was measured based on the reduction of NAD^+ to NADH, following the manufacturer's instructions.[43] NADH was measured spectrophotometrically at 450 nm at room temperature and the results expressed as change of absorbance per min per mg of protein.

Lactate measurement

In vitro lactate production of whole kidney homogenates from WKY and SHR was assayed spectrophotometrically at 450 nm at room temperature using a commercial lactate assay kit (BioVision, Mountain View, CA), following the manufacturer's instruction.

Blood pressure measurement

Fourteen day-old male SHR and WKY (as normotensive age- and sex-matched control) littermates were housed with their mothers in a facility accredited by the American Association for Accreditation of Laboratory Animal Care. At three-weeks of age, the littermates were weaned and caged individually. The littermates from both WKY and SHR were equally divided into two groups: Group 1, control rats (distilled water) and group 2, rats receiving DCA (0.75g/l) [44] in the drinking distilled water. Conscious rats were trained for non invasive blood pressure measurement at 37°C pre warmed platform, using the tail-cuff method (BP-2000 system, Visitech, Apex, NC), daily for 5 days from 17 days to 21 days of age (Supplementary Figure S4). After this training period BP reading were recorded and analyzed. For each blood pressure determination, twenty readings were obtained. The first 10 cycles were considered to be preliminary measurements and were not used for analysis; the remaining 10 readings, if obtained without technical problems such as excessive physical movements, were analyzed.

Statistical analysis

Data are presented as mean ± standard deviation (SD), unless stated otherwise. Significant differences between 2 groups were determined by Student's *t*-test. Significant differences among 3 or more groups were determined by factorial ANOVA, followed by Newman-Keuls test; $P<0.05$ was considered significant; analyses used SigmaStat 3.5 (SPSS Inc, Chicago, IL).

Supplementary Material

Refer to Web version on PubMed Central for supplementary material.

Acknowledgments

We are grateful to Drs. Jürgen Schnermann and Oksana Gavrilova (National Institute of Diabetes and Digestive and Kidney Diseases, National Institutes of Health, Bethesda, MD), and Dr. Cinthia B. Drachenberg (University of Maryland School of Medicine, Baltimore, MD) for their critical evaluation of the manuscript, Drs. Hideko Takahashi, Osama Ichii, Huiyan Lu, Patrick Dummer, Taichi Murakami, Hidefumi Wakashin, Koji Okamoto, Crisanto Escano, Peiying Yu, Perry Comegys, Norma Colocho, Kevin Bittman, and Margaret Finesilver for technical help. This study was supported in part by grants from the National Institutes of Health (R37HL023081, R01DK039308, R01HL092196, P01HL074940, and P01HL068686, P.A.J.), National Institute of Diabetes and Digestive and Kidney Diseases Intramural Research Program (Z01DK043308, J.B.K.), and Children's National Medical Center intramural Avery Award (H.L.).

References

1. Felder RA, White MJ, Williams SM, et al. Genetics of salt-sensitive hypertension. Curr Opin Nephrol Hypertens. 2013; 22:65–76. [PubMed: 23197156]
2. Kopp JB. Rethinking hypertensive kidney disease: arterionephrosclerosis as a genetic, metabolic, and inflammatory disorder. Curr Opin Nephrol Hypertens. 2013; 22:266–272. [PubMed: 23470819]
3. Herrera M, Coffman TM. The kidney and hypertension: novel insights from transgenic models. Curr Opin Nephrol Hypertens. 2012; 21:171–178. [PubMed: 22274801]
4. Zhang MZ, Yao B, Wang S, et al. Intrarenal dopamine deficiency leads to hypertension and decreased longevity in mice. J Clin Invest. 2011; 121:2845–2854. [PubMed: 21701066]
5. Gurley SB, Riquier-Brison AD, Schnermann J, et al. AT_{1A} angiotensin receptors in the renal proximal tubule regulate blood pressure. Cell Metab. 2011; 13:469–475. [PubMed: 21459331]
6. Wilcox CS. Oxidative stress and nitric oxide deficiency in the kidney: a critical link to hypertension? Am J Physiol Regul Integr Comp Physiol. 2005; 289:R913–R935. [PubMed: 16183628]
7. Li H, Han W, Villar VA, et al. D_1-like receptors regulate NADPH oxidase activity and subunit expression in lipid raft microdomains of renal proximal tubule cells. Hypertension. 2009; 53:1054–1061. [PubMed: 19380616]
8. Zou AP, Cowley AW Jr. Reactive oxygen species and molecular regulation of renal oxygenation. Acta Physiol Scand. 2003; 179:233–241. [PubMed: 14616239]
9. Zhang A, Jia Z, Wang N, et al. Relative contributions of mitochondria and NADPH oxidase to deoxycorticosterone acetate-salt hypertension in mice. Kidney Int. 2011; 80:51–60. [PubMed: 21368743]
10. Graham D, Huynh NN, Hamilton CA, et al. Mitochondria-targeted antioxidant $MitoQ_{10}$ improves endothelial function and attenuates cardiac hypertrophy. Hypertension. 2009; 54:322–328. [PubMed: 19581509]
11. Tian Z, Liu Y, Usa K, et al. Novel role of fumarate metabolism in Dahl-salt sensitive hypertension. Hypertension. 2009; 54:255–260. [PubMed: 19546378]
12. Welch WJ, Baumgartl H, Lubbers D, et al. Nephron pO_2 and renal oxygen usage in the hypertensive rat kidney. Kidney Int. 2001; 59:230–237. [PubMed: 11135075]
13. Brazy PC, Klotman PE. Increased oxidative metabolism in renal tubules from spontaneously hypertensive rats. Am J Physiol. 1989; 257:F818–F825. [PubMed: 2589484]
14. Stacpoole PW. The pyruvate dehydrogenase complex as a therapeutic target for age-related diseases. Aging Cell. 2012; 11:371–377. [PubMed: 22321732]
15. Holness MJ, Sugden MC. Regulation of pyruvate dehydrogenase complex activity by reversible phosphorylation. Biochem Soc Trans. 2003; 31:1143–1151. [PubMed: 14641014]
16. Abe Y, Sakairi T, Kajiyama H, et al. Bioenergetic characterization of mouse podocytes. Am J Physiol Cell Physiol. 2010; 299:C464–C476. [PubMed: 20445170]
17. Beeson CC, Beeson GC, Schnellmann RG. A high-throughput respirometric assay for mitochondrial biogenesis and toxicity. Anal Biochem. 2010; 404:75–81. [PubMed: 20465991]
18. Woost PG, Orosz DE, Jin W, et al. Immortalization and characterization of proximal tubule cells derived from kidneys of spontaneously hypertensive and normotensive rats. Kidney Int. 1996; 50:125–134. [PubMed: 8807581]

19. Okamoto K, Aoki K. Development of a strain of spontaneously hypertensive rats. Jpn Circ J. 1963; 27:282–293. [PubMed: 13939773]
20. Gray SD. Pressure profiles in neonatal spontaneously hypertensive rats. Biol Neonate. 1984; 45:25–32. [PubMed: 6692014]
21. Felder RA, Kinoshita S, Ohbu K, et al. Organ specificity of the dopamine1 receptor/adenylyl cyclase coupling defect in spontaneously hypertensive rats. Am J Physiol. 1993; 264:R726–732. [PubMed: 8476116]
22. Padmanabhan S, Newton-Cheh C, Dominiczak AF. Genetic basis of blood pressure and hypertension. Trends Genet. 2012; 28:397–408. [PubMed: 22622230]
23. Cowley AW Jr, Nadeau JH, Baccarelli A, et al. Report of the National Heart, Lung, and Blood Institute Working Group on epigenetics and hypertension. Hypertension. 2012; 59:899–905. [PubMed: 22431584]
24. He W, Miao FJ, Lin DC, et al. Citric acid cycle intermediates as ligands for orphan G-protein-coupled receptors. Nature. 2004; 429:188–193. [PubMed: 15141213]
25. de Cavanagh EM, Toblli JE, Ferder L, et al. Renal mitochondrial dysfunction in spontaneously hypertensive rats is attenuated by losartan but not by amlodipine. Am J Physiol Regul Integr Comp Physiol. 2006; 290:R1616–R1625. [PubMed: 16410402]
26. Postnov YV, Orlov SN, Budnikov YY, et al. Mitochondrial energy conversion disturbance with decrease in ATP production as a source of systemic arterial hypertension. Pathophysiology. 2007; 14:195–204. [PubMed: 17949954]
27. Phillips D, Covian R, Aponte AM, et al. Regulation of oxidative phosphorylation complex activity: effects of tissue-specific metabolic stress within an allometric series and acute changes in workload. Am J Physiol Regul Integr Comp Physiol. 2012; 302:R1034–R1048. [PubMed: 22378775]
28. Calderón-Cortés E, Cortés-Rojo C, Clemente-Guerrero M, et al. Changes in mitochondrial functionality and calcium uptake in hypertensive rats as a function of age. Mitochondrion. 2008; 8:262–272. [PubMed: 18541459]
29. Li XX, Xu J, Zheng S, et al. D1 dopamine receptor reglation of NHE3 during development in spontaneously hypertensive rats. Am J Physiol Regul Integr Comp Physiol. 2001; 280:R11650–R1656.
30. Crajoinas RO, Lessa LM, Carraro-Lacroix LR, et al. Posttranslational mechanisms associated with reduced NHE3 activity in adult vs. young prehypertensive SHR. Am J Physiol Renal Physiol. 2010; 299:F872–F881. [PubMed: 20630932]
31. Morduchowicz GA, Sheikh-Hamad D, Jo OD, et al. Increased Na^+/H^+ antiport activity in the renal brush border membrane of SHR. Kidney Int. 1989; 36:576–581. [PubMed: 2554051]
32. Zheleznova NN, Yang C, Ryan RP, et al. Mitochondrial proteomic analysis reveals deficiencies in oxygen utilization in medullary thick ascending limb of Henle in the Dahl salt-sensitive rat. Physiol Genomics. 2012; 44:829–842. [PubMed: 22805345]
33. Colombini M. Mitochondrial outer membrane channels. Chem Rev. 2012; 112:6373–6387. [PubMed: 22979903]
34. Raschle T, Hiller S, Yu TY, et al. Structural and functional characterization of the integral membrane protein VDAC-1 in lipid bilayer nanodiscs. J Am Chem Soc. 2009; 131:17777–17779. [PubMed: 19916553]
35. Palm F, Nordquist L. Renal oxidative stress, oxygenation, and hypertension. Am J Physiol Regul Integr Comp Physiol. 2011; 301:R1229–R1241. [PubMed: 21832206]
36. Zeng C, Villar VA, Yu P, et al. Reactive oxygen species and dopamine receptor function in essential hypertension. Clin Exp Hypertens. 2009; 31:156–178. [PubMed: 19330604]
37. Doughan AK, Harrison DG, Dikalov SI. Molecular mechanisms of angiotensin II-mediated mitochondrial dysfunction: linking mitochondrial oxidative damage and vascular endothelial dysfunction. Circ Res. 2008; 102:488–496. [PubMed: 18096818]
38. Shen YC, Ou DL, Hsu C, et al. Activating oxidative phosphorylation by a pyruvate dehydrogenase kinase inhibitor overcomes sorafenib resistance of hepatocellular carcinoma. Br J Cancer. 2013; 108:72–81. [PubMed: 23257894]

39. Michelakis ED, Sutendra G, Dromparis P, et al. Metabolic modulation of glioblastoma with dichloroacetate. Sci Transl Med. 2010; 2:31ra34.

40. Papadimitriou JC, Drachenberg CB, Shin ML, et al. Ultrastructural studies of complement mediated cell death: a biological reaction model to plasma membrane injury. Virchows Arch. 1994; 424:677–685. [PubMed: 8055163]

41. Reja V, Goodchild AK, Pilowsky PM. Catecholamine-related gene expression correlates with blood pressure in SHR. Hypertension. 2002; 40:342–347. [PubMed: 12215477]

42. Lee I, Salomon AR, Ficarro S, et al. cAMP-dependent tyrosine phosphorylation of subunit I inhibits cytochrome c oxidase activity. J Biol Chem. 2005; 280:6094–6100. [PubMed: 15557277]

43. Jeoung NH, Sanghani PC, Zhai L, et al. Assay of the pyruvate dehydrogenase complex by coupling with recombinant chicken liver arylamine N-acetyltransferase. Anal Biochem. 2006; 356:44–50. [PubMed: 16859625]

44. McMurtry MS, Bonnet S, Wu X, et al. Dichloroacetate prevents and reverses pulmonary hypertension by inducing pulmonary artery smooth muscle cell apoptosis. Circ Res. 2004; 95:830–840. [PubMed: 15375007]

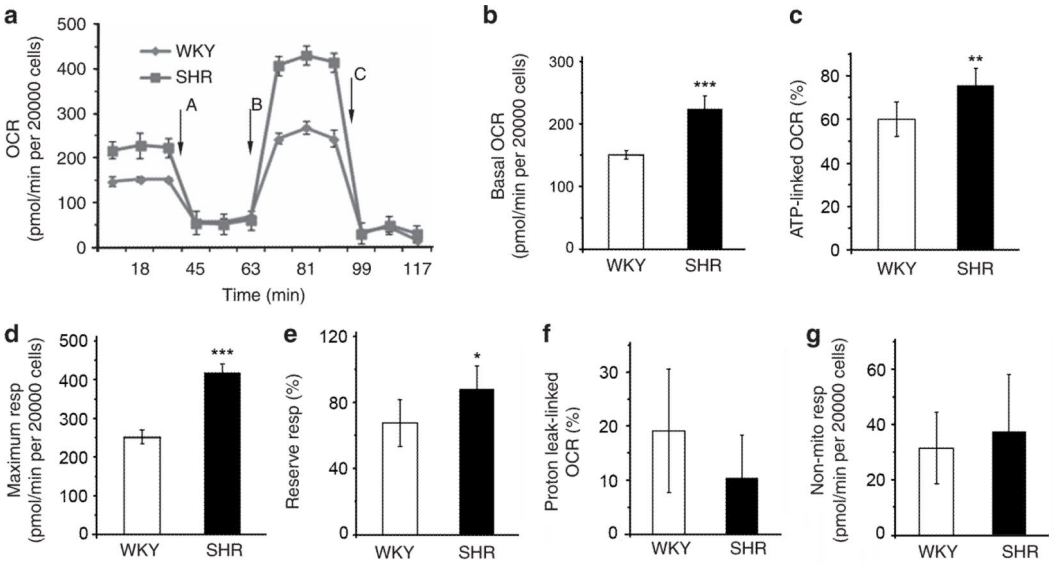

Figure 1. Bioenergetics profiles of renal proximal tubule cells in primary culture from WKY and SHR

(a) OCR tracings from renal proximal tubule cells in primary culture from WKY and SHR; error bars are SD from readings from 3 wells. Cells were sequentially exposed to oligomycin (arrow A), FCCP (arrow B), and the combination of rotenone and antimycin A (arrow C), via the reagent delivery chambers of the sensor cartridge. n=8-9, *P<0.05, **P<0.01, ***P<0.001, vs. WKY, Student's *t*-test. **(b)** Basal OCR was calculated as the OCR prior to the injection of oligomycin. **(c)** ATP synthesis-linked OCR (ATP-linked OCR) was calculated as the basal OCR minus the nadir following oligomycin. **(d)** Maximum respiration (Maximum resp) was defined as the peak OCR following the injection of FCCP. **(e)** Reserve respiration (Reserve resp) was defined as the difference between maximum respiration and basal OCR. **(f)** Proton leak-linked OCR was defined as the difference between uncoupled respiration following oligomycin and non-mitochondrial respiration following the injection of rotenone and antimycin A. **(g)** Non-mitochondrial respiration (Non-mito resp) was defined as the OCR following the injection of rotenone and antimycin A.

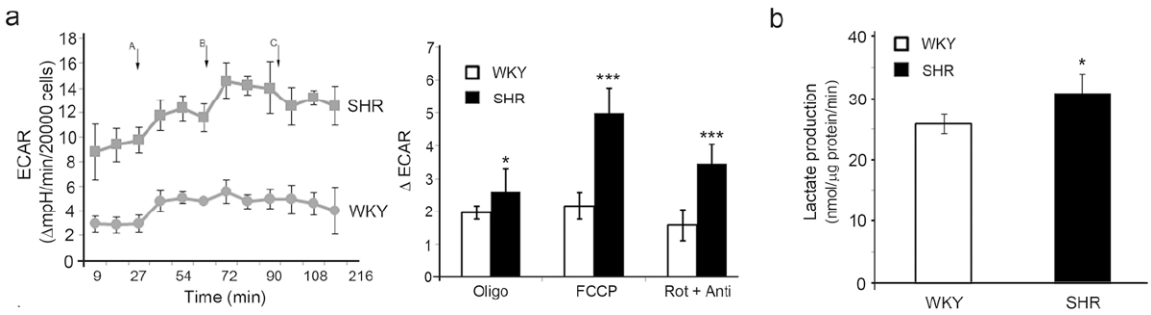

Figure 2. Extracellular acidification rate (ECAR) and lactate production in WKY and SHR

(a) ECAR was measured, in parallel with OCR, following the sequential injections of oligomycin (arrow A), FCCP (arrow B), and the combination of rotenone and antimycin A (arrow C); graphs of tracings are shown with SD of readings from 3 wells. Higher ECAR value indicates reduction in pH and increase in glycolysis. Comparison of the change in ECAR from baseline after injection of mitochondrial inhibitors is plotted, n=12-16, * P<0.05, ***P<0.001 Student's *t*-test. Each group included 3 replicates. Oligo, oligomycin; FCCP, carbonilcyanide p-trifluoromethoxyphenylhydrazone; Rot, rotenone; Anti, antimycin A. **(b)** Lactate production was measured in whole kidney homogenates from WKY and SHR. n=6, *P<0.05 vs. WKY, Student's *t*-test.

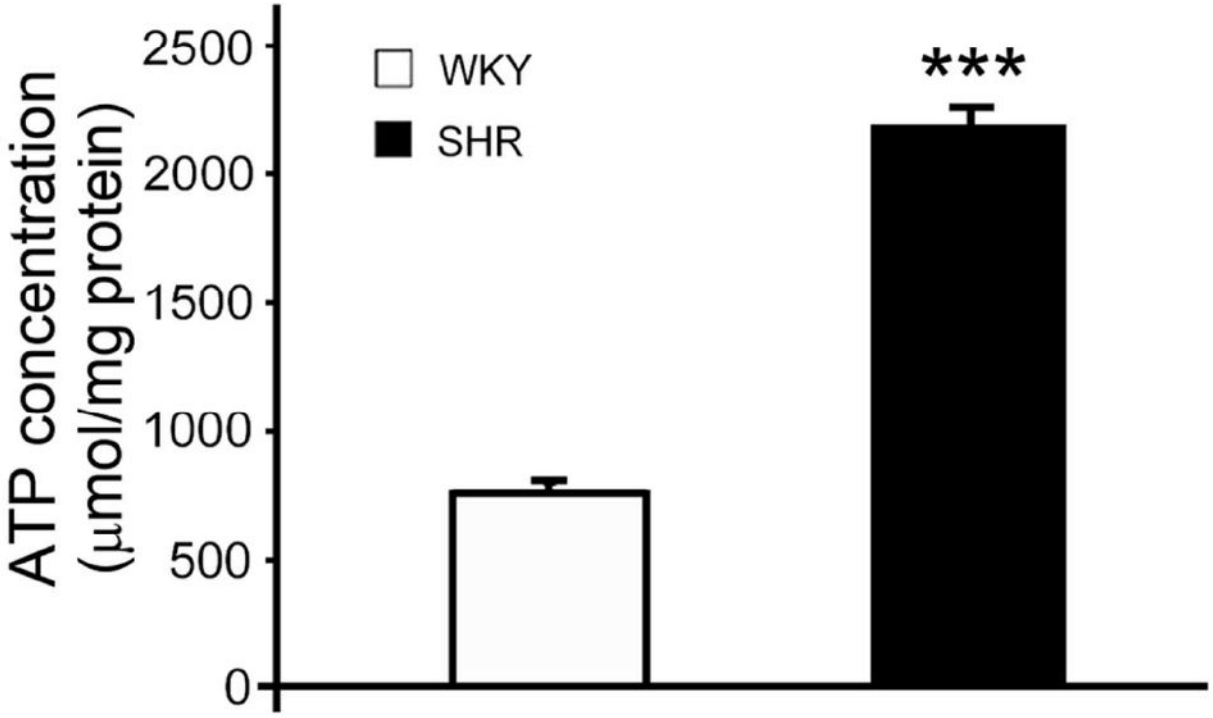

Figure 3. Intracellular ATP concentration in renal proximal tubule cells from WKY and SHR

Fully confluent renal proximal tubule cells from WKY and SHR were harvested, pelleted, and lysed. ATP was released in 300 μl of boiling buffer with continued boiling for 2 min as described in the Methods section, and ATP concentration was quantified by bioluminescence. n=3, ***P<0.001 vs. WKY, Student's *t*-test.

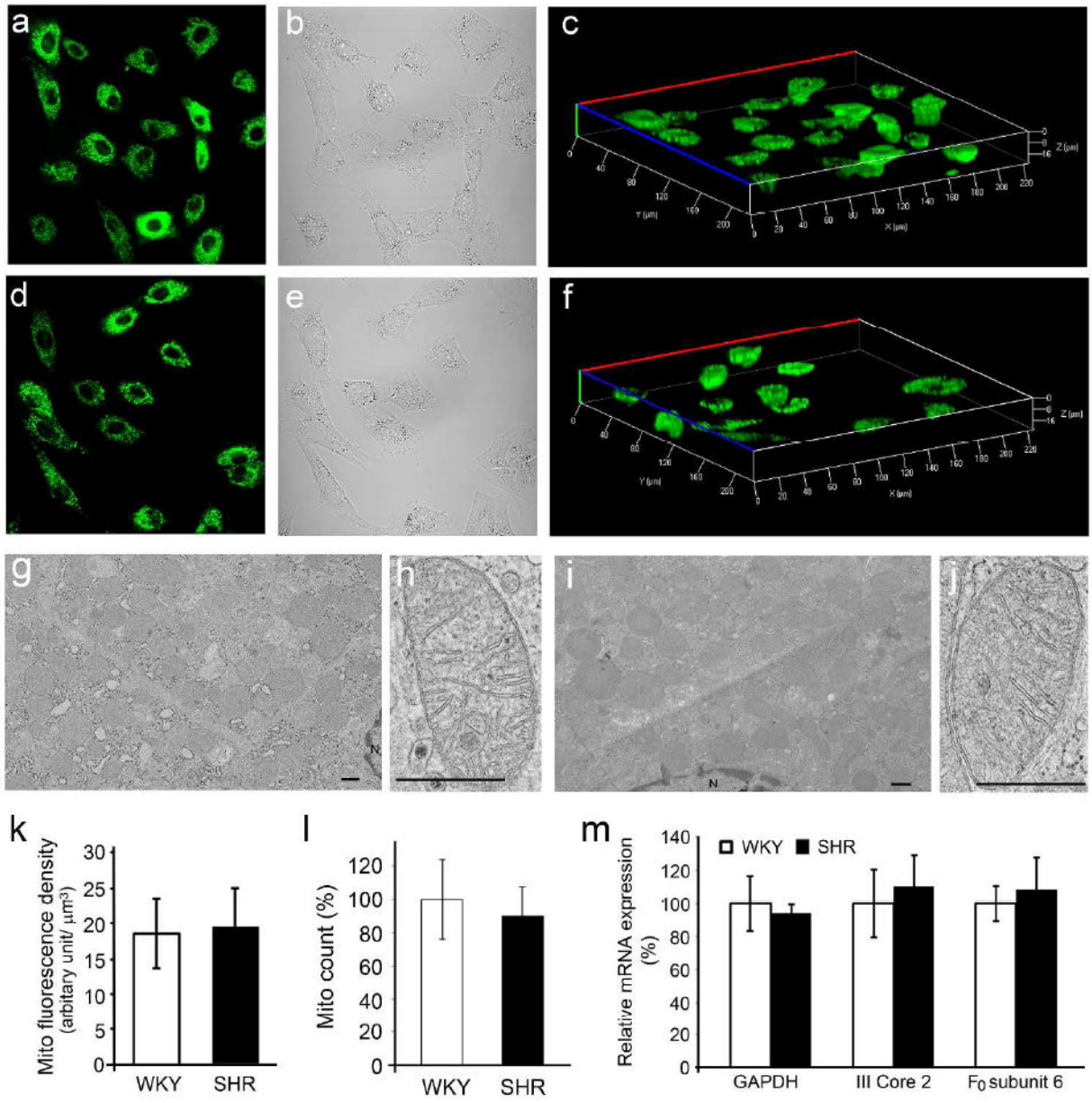

Figure 4. Mitochondrial characteristics in renal proximal tubule cells from WKY and SHR

Live renal proximal tubule cells in primary culture from WKY **(a-c)** and SHR **(d-f)** were stained with MitoTracker Green. A representative mitochondrial staining (**a** and **d**), differential interference contrast or DIC (**b** and **e**) in the focal plane, and their 3D images (**c** and **f**) are shown. 3D reconstruction and imaging analysis were conducted using the built-in Zen 2011 software. The MitoTracker fluorescence density, which was calculated from 26-37 cells in each of three independent experiments, was not different (P>0.05, Student's *t*-test) between WKY and SHR (**k**). Electron microscopy showed that the distribution of mitochondria (**g, i**), intact folded cristae, and inner and outer membrane structures (**h, j**) in renal proximal tubule cells were similar in WKY (**g, h**) and SHR (**i, j**), bar, 500 nm; N, nucleus (**g, i**). The abundance of mitochondria (**l**) (randomly counted from 15-20 fields for

each section at 3,000× magnification) was similar (P>0.05, Student's *t*-test) in WKY and SHR. The mRNA expressions of GAPDH, Complex III core 2 (III Core 2), and ATP synthase F_0 subunit 6 (F_0 subunit 6), measured by quantitative real-time PCR (qRT-PCR) and normalized to 18S rRNA (**m**), were similar in WKY and SHR; the individual gene expression in renal proximal tubule cells from WKY was considered as 100%, n = 3 per group, P>0.05, ANOVA, Newman-Keuls test.

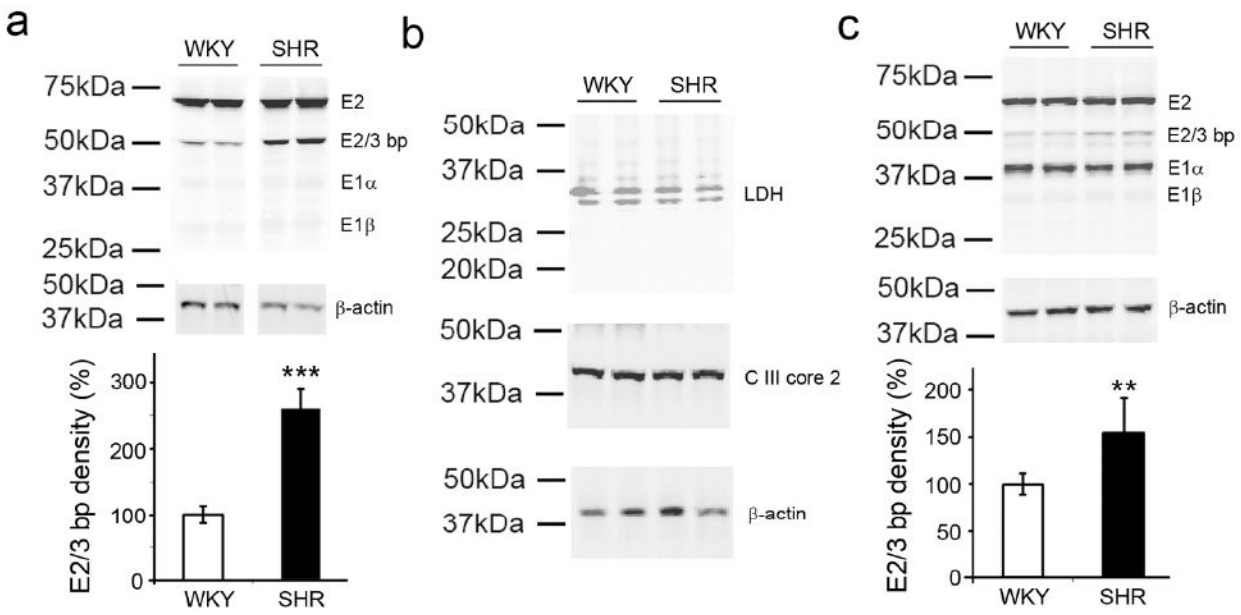

Figure 5. Pyruvate dehydrogenase complex protein expression in renal proximal tubule cells and renal cortical homogenates from WKY and SHR

(**a**) Renal proximal tubule cell lysates from WKY and SHR were separated by electrophoresis and immunoblotted with pyruvate dehydrogenase complex antibody cocktail. β-actin was used for protein loading control. The density of pyruvate dehydrogenase complex E2/3 binding protein subunit was quantified by densitometry and normalized to that of WKY lysates (lower panel). The proteins were run on the same gel but were noncontiguous, n = 5-7, ***P < 0.001 vs. WKY, Student's *t*-test. E2/3 bp, E2/3 binding protein.

(**b**) The same cell lysates from (**a**) were electrophoresed and immunoblotted with anti-LDH, anti-complex III core 2, and anti-β-actin antibodies. LDH, lactate dehydrogenase; C III core 2, Complex III core 2 protein.

(**c**) Renal cortical homogenate proteins from WKY and SHR were separated by electrophoresis and immunoblotted with pyruvate dehydrogenase complex antibody cocktail and anti-β-actin for protein loading control. The density of pyruvate dehydrogenase complex E2/3 bp subunit proteins was quantified by densitometry and normalized to that of WKY, n = 8, **P<0.01 vs. WKY, Student's *t*-test.

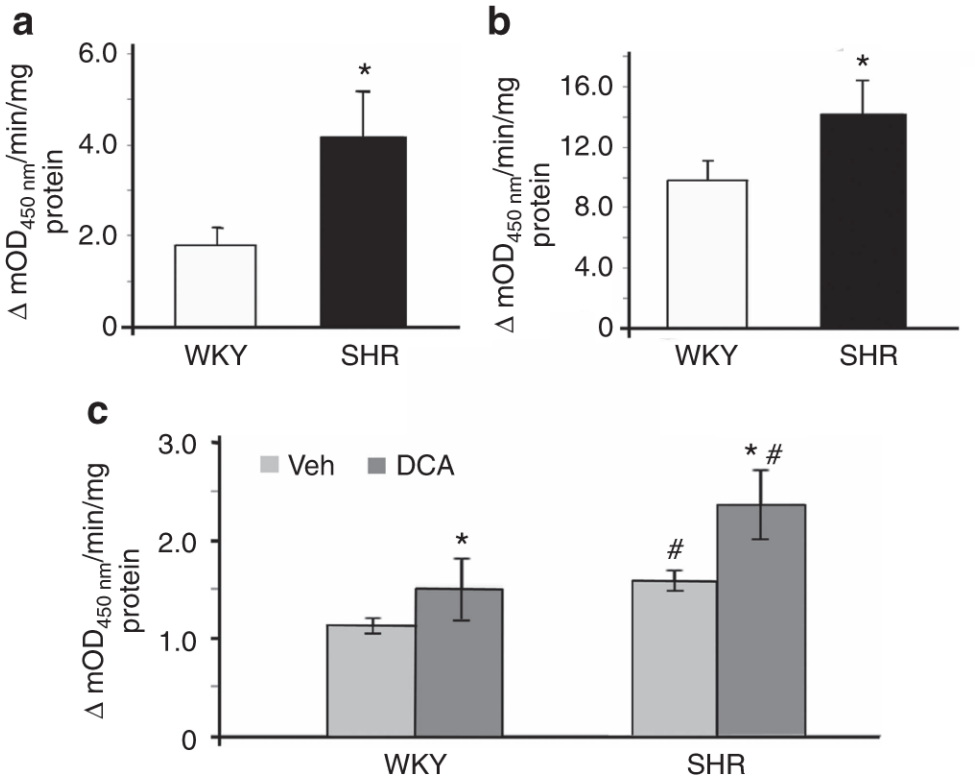

Figure 6. Pyruvate dehydrogenase complex activity in WKY and SHR

Specific pyruvate dehydrogenase complex activity was determined by a spectrophotometric method. **(a)** Renal proximal tubule cell lysates from WKY and SHR, n=3, *P< 0.05 vs. WKY, Student's *t*-test. (**b**) Renal cortical tissue homogenates from WKY and SHR. n = 6, *P < 0.05 vs. WKY, Student's *t*- test. (**c**) Whole kidney homogenates from WKY and SHR treated with vehicle or DCA. n = 6-9, *P < 0.05 vs. vehicle, # P<0.05 vs. WKY, ANOVA, Dunn's test. Error bars are SD.

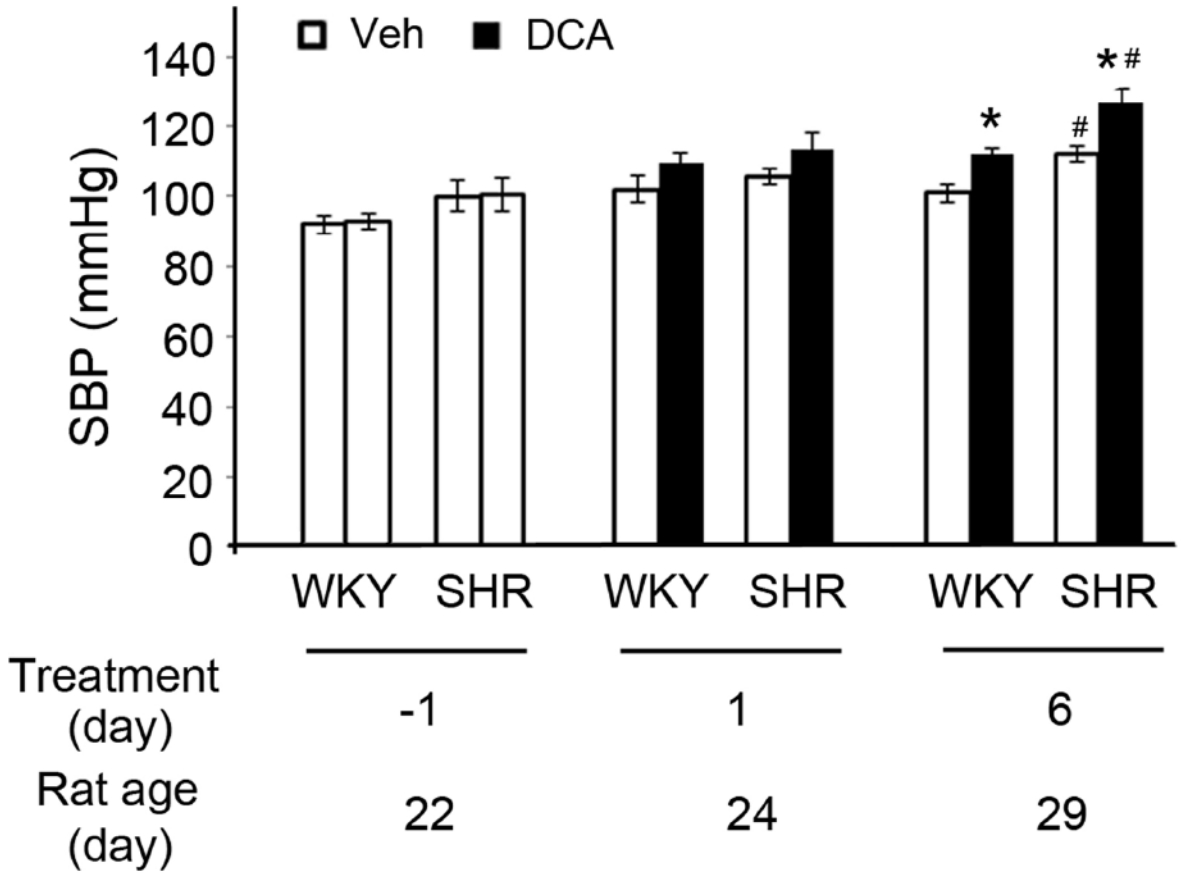

Figure 7. Effect of DCA on blood pressure in young WKY and SHR

Vehicle (Veh) or DCA was administered via the drinking water, which was changed every other day for 6 days. Systolic blood pressure (SBP) was measured by tail-cuff method. n = 9-11. *P < 0.05, *P<0.05 DCA vs. Veh, #P<0.05 SHR vs. WKY, ANOVA, Newman-Keuls test. Data are mean ± SEM.